JOURNAL OF MATERIALS SCIENCE 24 (1989) 1316–1322

Deformation mechanisms in toughened poly(phenylene oxide)–polyamide blends

S. Y. HOBBS, M. E. J. DEKKERS
Polymer Physics and Engineering Laboratory, Corporate Research and Development, General Electric Company, Schenectady, New York 12301, USA

The deformation behaviour of several toughened poly(phenylene oxide)–Nylon 6,6 blends made with different coupling agent levels and having different copolymer concentrations has been studied by tensile dilatometry and scanning electron microscopy. Volume strains were measured at rates from 10^{-3} to 10^{-1} sec^{-1}. At high copolymer concentrations, shearing was the primary deformation mode with dilation accounting for only 25% of the total strain. At lower copolymer levels, fracture occurred abruptly with no measurable increase in the level of cavitation prior to failure. Samples without rubber exhibited lower levels of dilation than their toughened counterparts. The observed differences in behaviour are discussed in terms of microscopic failure processes in the materials. Rate-dependent values for selected engineering parameters are presented.

1. Introduction

The impact performance and morphology of toughened blends of poly(phenylene oxide) and Nylon 6,6 made with different levels of coupling agent and having different copolymer concentrations have been discussed in some detail [1]. It has been shown that in blends having high copolymer concentrations, progressive softening of the dispersed poly(phenylene oxide) phase by the addition of rubber produces significant increases in the local stress field intensities around these microscopic inclusions. This change lessens the effect of fortuitous stress risers and increases the toughness of the blend by delocalizing the deformation more uniformly throughout the material. It is the objective of this study to consider the deformation behaviour of these materials in more detail.

Volume dilatometry was chosen as the primary tool for evaluating the macroscopic deformation behaviour of the poly(phenylene oxide)–Nylon 6,6 blends. By simultaneously measuring the axial and transverse strains on a sample placed in uniaxial tension, the volume strain, and, hence, the contribution of dilative processes, such as crazing and debonding, to the deformation behaviour can be measured [2–4]. The extent to which these parameters are affected by the rate of deformation and the composition of the resin can also be determined.

Unfortunately, from these experiments, it is not possible to discriminate between the various cavitation processes which may play a role or to determine how these may be localized within a test specimen. To circumvent this deficiency, electron microscopy was used to characterize selected specimens from the volume strain experiments and impact strength tests. Several previously unexpected features of the deformation process were identified in this fashion and are described in the following text.

2. Experimental details

Samples used in this study were prepared and stored as described previously [1]. Unless otherwise noted, the poly(phenylene oxide)–Nylon 6,6–impact modifier ratio was fixed at 50 : 40 : 10 parts by weight. Coupling agent levels were adjusted to produce copolymer concentrations in the range 0 to ~30% by weight. In addition to these samples, an identical blend containing 3% TiO_2 pigment and another having a copolymer concentration of 20% but no impact modifier were prepared.

Tensile stress–strain–volume strain (σ–ε–($\Delta V/V$)) experiments were carried out on an Instron 1350 servo-hydraulic testing machine at rates ranging from 10^{-3} to 10^{-1} sec^{-1}. Volume changes were measured using nested axial and transverse strain gauges affixed to the samples as shown in Fig. 1. The gauges were calibrated over strain ranges of 0 to 14% and 0 to 5% respectively and found to be linear. All testing was done in strain control using the output of the axial strain gauge to control the crosshead displacement rate.

The outputs from the load, axial strain, transverse strain, and stroke channels were collected using a Norland 3001 processing digital oscilloscope. Intermediate processing of the data was carried out on the Norland to compute values for the applied stress and volume strain. The converted data were then transferred as ASCII files to the mass storage device of an HP 9826 mini computer. All further manipulation of the data was carried out on the HP using "Basic" programs to calculate the best least square values for Poisson's ratio and Young's modulus over selected

0022–2461/89 $03.00 + .12

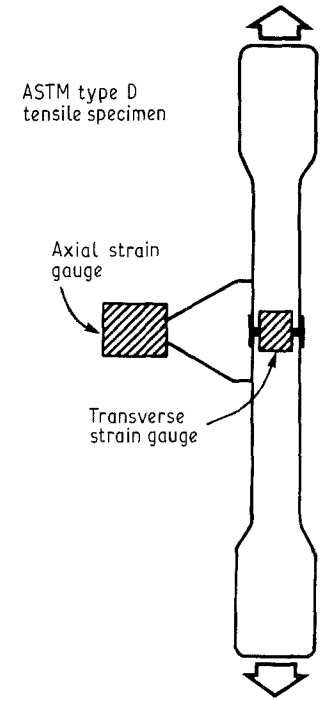

Figure 1 Testing configuration for volume strain measurements.

axial strain ranges. σ–ε–$(\Delta V/V)$ plots were made using an HP 7475A pen plotter.

In those samples to be examined by scanning electron microscopy, the surface skin produced during injection moulding was removed prior to testing. The specimens were then strained in uniaxial tension, removed from the Instron, bent slightly to place the surface of interest in tension, and immersed in 1% aqueous osmium tetroxide. This procedure proved effective in stabilizing the deformed regions which tended to collapse when stress was removed from the test specimens. After removal from the osmium textroxide solution, small sections were cut from the bars, microtomed, sputter coated with a Au–Pd alloy and examined using a JEOL 840 scanning electron microscope.

Samples for transmission electron microscopy were stained by immersion in a 1% osmium tetroxide solution in hexane for 2 h. Thin sections were cut at room temperature using a Reichart Ultracut E ultramicrotome and examined using a Hitachi H-600 TEM.

3. Results

3.1. Volume strain studies

All of the materials having more then 15% copolymer were found to deform in a ductile fashion up to 14% strain over the entire range of strain rates from 10^{-3} to $10^{-1}\,\text{sec}^{-1}$. A typical example is shown in Fig. 2. Over this range of compositions, changes in the copolymer level produced no significant variations in the stress–strain–volume strain plots or the impact behaviour (see [1] and below). Both the engineering stress (σ_E) against strain curves and the true stress (σ_T) against strain curves began to plateau at approximately 4% strain without showing a well-defined yield point. Necking was absent and there was significant stress whitening and increased surface gloss in each of the gauge sections. Initially, all of the volume strain curves exhibited a small positive slope due to the Poisson effect. The dilation became more pronounced above the linear elastic region (axial strain, $\varepsilon_A = 1.5\%$) and remained elevated until it reached 6 to 8%. At higher strains the slopes decreased to values close to those observed initially.

Samples moulded from the blend containing 10% copolymer survived the lowest strain rate tensile tests but exhibited occasional fractures between 10 and 14% strain at rates of 10^{-2} and $10^{-1}\,\text{sec}^{-1}$. Both the gauge sections and fracture surfaces showed extensive stress whitening. All of the blends containing lower levels of copolymer fractured at 2 to 3% strain at $10^{-3}\,\text{sec}^{-1}$ and were not tested at higher rates. Interrupted stress-whitened patches were visible on these fracture surfaces and subsurface satellite cracks could often be observed running at an angle to the primary fracture plane. Significantly, the volume strain curves for these blends were very similar to those exhibited by the blends containing higher copolymer levels with no marked increase in dilation preceding the failure. A typical σ–ε–$(\Delta V/V)$ plot for one of the specimens exhibiting low strain, brittle failure is shown in Fig. 3.

Elimination of the impact modifier markedly reduced the ductility of the blends especially at the higher strain rates. At strain rates of $10^{-3}\,\text{sec}^{-1}$ fracture was often observed at 6 to 8% strain. There was also a marked drop in the extent of cavitation at intermediate strains (2 to 6%) as compared with the toughened blends and no stress whitening was observed. The untoughened blends exhibited a corresponding increase in modulus and yield strength. All of these

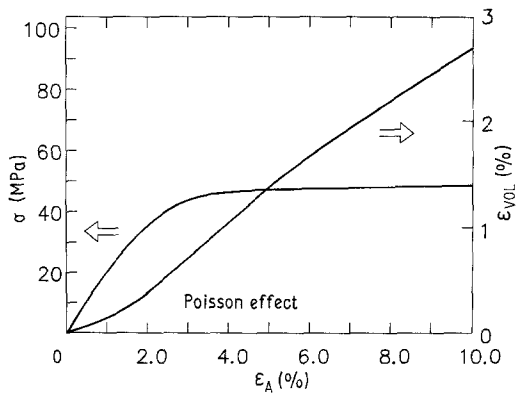

Figure 2 σ–ε–$(\Delta V/V)$ plots for a poly(phenylene oxide)–Nylon 6,6–rubber blend containing 20% copolymer tested at $10^{-3}\,\text{sec}^{-1}$.

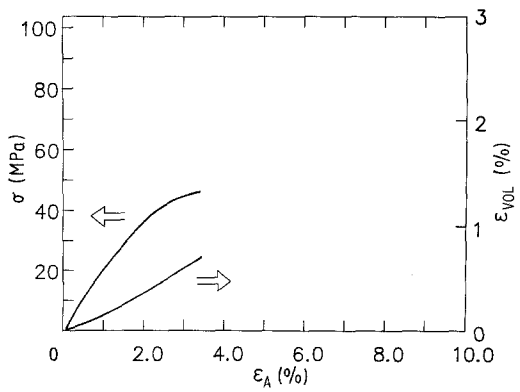

Figure 3 σ–ε–$(\Delta V/V)$ plots for a poly(phenylene oxide)–Nylon 6,6–rubber blend containing 7% copolymer tested at $10^{-3}\,\text{sec}^{-1}$.

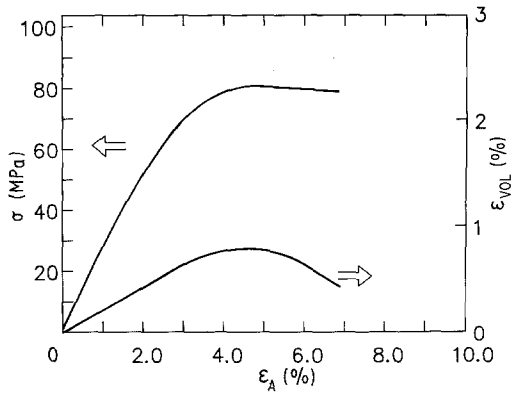

Figure 4 σ–ε–$(\Delta V/V)$ plots for a poly(phenylene oxide)–Nylon 6,6–blend containing 20% copolymer tested at $10^{-2}\,sec^{-1}$.

features are illustrated in Fig. 4. The observed differences were reflected in the notched Izod impact values which dropped from 150 to 170 J m^{-1} for the blends containing impact modifier to less than 30 J m^{-1} for those without.

The elastic, deviatoric (shear) and dilational (cavitation) contributions to the overall strain were calculated assuming that they were linearly additive [5, 6]. Although such a model has obvious deficiencies, it does provide a reasonable approximation for these parameters which is useful for comparison. The exact values should be treated with some caution. Using this approximation it can be shown that the individual strain components are given by the following expressions

$$\varepsilon_{EL} = \sigma_T/E \quad (1)$$

$$\varepsilon_{DIL} = \Delta V/V_0 - (1 - 2\nu)\sigma_T/E \quad (2)$$

$$\varepsilon_{DEV} = \varepsilon - \Delta V/V_0 - 2\nu\sigma_T/E \quad (3)$$

where ε_{EL}, ε_{DIL}, ε_{DEV} are the elastic, dilational and deviatoric strains, respectively and ν is Poisson's ratio.

Typical plots for a poly(phenylene oxide)–Nylon 6,6–rubber blend containing 23% copolymer which displayed ductile behaviour to 14% strain and a similar blend containing 7% copolymer which failed in a brittle fashion at 3.4% strain are shown in Figs 5 and 6. In both cases, the initial deformation is predominately elastic. As the strain increases, the onset of

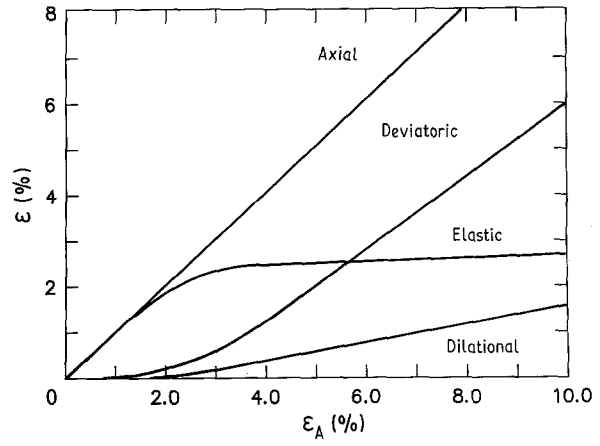

Figure 5 Plot showing the ε_{EL}, ε_{DIL}, and ε_{DEV} contributions to the total strain for a poly(phenylene oxide)–Nylon 6,6–rubber blend containing 28% copolymer and displaying ductile deformation at $10^{-3}\,sec^{-1}$.

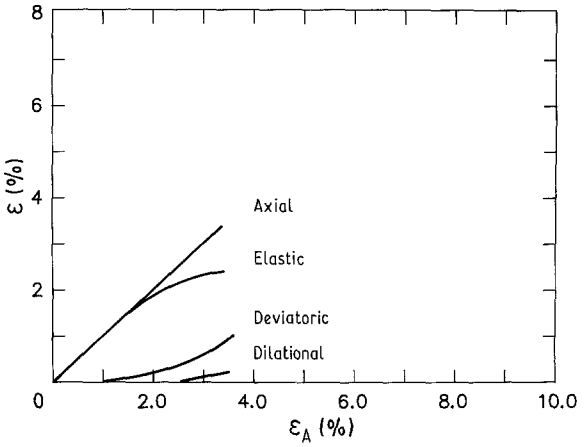

Figure 6 Plot showing the ε_{EL}, ε_{DIL}, and ε_{DEV} contributions to the total strain for a poly(phenylene oxide)–Nylon 6,6–rubber blend containing 7% copolymer and displaying brittle deformation at $10^{-3}\,sec^{-1}$.

shear flow (ε_A = 1.5%) precedes the onset of dilation (ε_A = 2%) and ultimately becomes the dominant deformation mechanism as the stress becomes constant. This behaviour was consistently observed for all of the resins with the exception of the blend containing pigment. In this material both the shear and dilative strains were observed to initiate at ε_A = 1.5% and to rise coincidently to ε_A = 2.5%. At this point, the slope of the $\varepsilon_{DEV}/\varepsilon_A$ curve began to increase more rapidly although the overall level of dilation remained higher than that of the unpigmented specimens. These differences suggest that significant debonding of the pigment particles occurs during the early stages of deformation.

It is illuminating to compare the deformation behaviour of a well-coupled, toughened blend with that of the Nylon matrix resin (see Fig. 7). The initial slope of the volume strain curve for Nylon 6,6 shows little deviation from linearity up to 1.5% strain. The elastic modulus is markedly higher than that for the blend while the Poisson ratios for the two materials are identical (see Table I). A small drop in $\Delta V/V$ is observed as the stress against strain curve begins to plateau. At higher strains, the specimens undergo plastic flow with no neck formation. The volume increases slightly during this time but reaches a maximum value less than 25% of that measured for the blend. Examination of the individual strain components for Nylon 6,6 (see Fig. 8) shows that deformation results almost entirely from elastic strain and

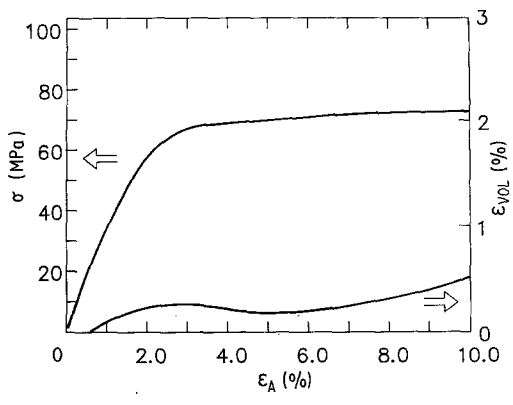

Figure 7 σ–ε–$(\Delta V/V)$ plots for Nylon 6,6 homopolymer tested at $10^{-3}\,sec^{-1}$

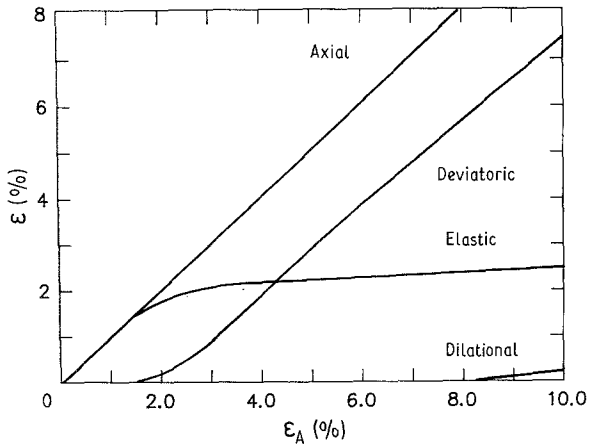

Figure 8 Plot showing the ε_{EL}, ε_{EL} and ε_{DEV} contributions to the total strain for Nylon 6,6 homopolymer specimen.

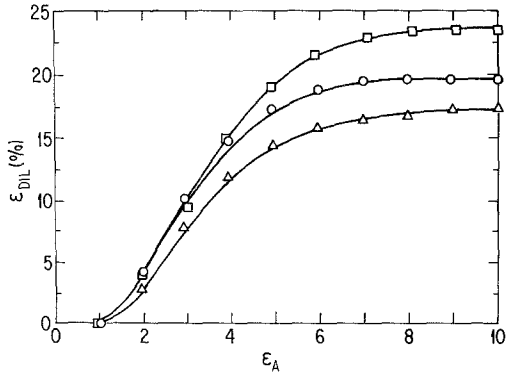

Figure 9 Variation in ε_{DIL} with ε_A for poly(phenylene oxide)–Nylon 6,6–rubber blends containing 15% copolymer (□ $10^{-1}\,sec^{-1}$, ○ $10^{-2}\,sec^{-1}$, △ $10^{-3}\,sec^{-1}$).

shear flow with minimal dilation. No stress whitening was observed in the Nylon 6,6 homopolymer.

The rate-dependent modulus, yield stress, and Poisson ratio values (the latter extracted from linear regions of the $\Delta V/V$ curves) for the resins used in this study are listed in Table I. In Fig. 9 the dilative components of the total strain are plotted as a function of strain rate for the specimens containing 15% copolymer. Moderate increases in the ultimate values of ε_{DIL} are noted although the low strain values are very similar. The curves for the other unpigmented resins were similar while the maximum ε_{DIL} values for the pigmented resin were 5% higher. The variations in engineering yield stress (4% strain) with strain rate are plotted in Fig. 10 for blends having two different copolymer concentrations. Above 15% the slope of the engineering yield stress (4% strain), σ_{ey} against strain rate, $\dot{\varepsilon}$ curve was found to be insensitive to copolymer level.

4. Microscopic analysis

SEM photomicrographs of a poly(phenylene oxide)–Nylon 6,6–rubber blend containing 20% copolymer and taken to 10% strain are presented in Figs. 11 and 12. From these pictures it is evident that cavitation is concentrated almost exclusively within the poly(phenylene oxide) phase and to a much lesser extent at the poly(phenylene oxide)–Nylon 6,6 interface. There is no evidence of crazing or void formation in the Nylon resin. The cavitated domains are organized into "macro crazes" which range between 5 and 10 μm in thickness and extend for much larger distances in lateral dimensions. The intervening nylon matrix in these regions appears to have undergone sufficient plastic deformation to accommodate the increase in volume associated with cavitation of the dispersed phase.

Transmission electron microscopy provides strong evidence that a significant fraction of the voids in the poly(phenylene oxide) phase results from internal cavitation of the rubber. A photomicrograph taken from an area just below the fracture surface of an Izod bar failing at 150 J m^{-1} is presented in Fig. 13. The cavitated regions within the rubber phase are clearly evident. In order to insure that the rubber was not damaged during microtomy, thin sections were cut from an undeformed bar and examined in the same fashion. In each case the stained rubber particles were intact with no evidence of internal or interfacial voiding.

In contrast to the toughened blends, those without rubber showed no evidence of cavitation within the poly(phenylene oxide) domains at deformation rates

TABLE I

($\dot{\varepsilon}$ = $10^{-3}\,sec^{-1}$)	σ_{EY} (MPa) (ε_A = 4%)	E (MPa) (ε_A = 0.1–0.7%)	$\Delta V/V/\varepsilon$		
			(ε_A = 0.1–0.7%)	(ε_A = 2–4%)	(ε_A = 6–10%)
Nylon 6,6 (0.12% H_2O)	–	3200 ± 144	0.42	–	–
Nylon 6,6 (1.2%, H_2O)	–	2537 ± 75	0.48	–	–
Blend:					
0% Copolymer	41.8 ± 0.9	2082 ± 35	0.44	0.37*	–
15% Copolymer	48.3 ± 1.1	2027 ± 28	0.43	0.39	0.40
28% Copolymer ($\dot{\varepsilon}$ = $10^{-2}\,sec^{-1}$)	48.7 ± 0.1	2068 ± 28	0.41	0.37	0.40
Blend					
0% Copolymer	40.1 ± 0.4	2027 ± 27	0.44	0.32*	–
15% Copolymer	52.3 ± 0.3	2179 ± 14	0.44	0.34	0.38
28% Copolymer ($\dot{\varepsilon}$ = $10^{-1}\,sec^{-1}$)	53.5 ± 0.1	2193 ± 21	0.43	0.34	0.39
Blend					
0% Copolymer	–	–	–	–	–
15% Copolymer	55.7 ± 0.3	2213 ± 7	0.42	0.34	0.34
28% Copolymer	56.8 ± 0.6	2241 ± 7	0.42	0.32	0.38

*Sample fractured.

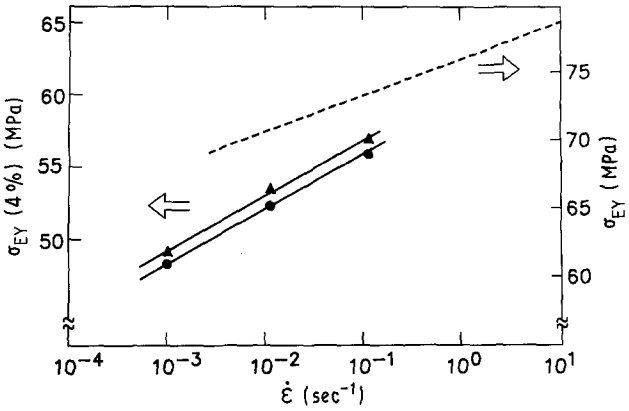

Figure 10 Yield stress (4% strain) plotted against log ($\dot{\varepsilon}$) for unpigmented poly(phenylene oxide)–Nylon 6,6–rubber blends containing 15% (●) and 28% (▲) copolymer. Upper line (– – –) is a replot of data for Nylon 6,6 taken from Hartman and Cole [8].

up to $10^{-1}\,\mathrm{sec}^{-1}$. A photomicrograph near a crack tip in such a specimen containing 20% coupling agent and strained to 5% in uniaxial tension is shown in Fig. 14. The area of plastic deformation next to the growing crack is clearly visible. In this well-coupled blend the two components deform in concert over most of the plastic zone although isolated interfacial voids are occasionally visible adjacent to the crack. These eventually combine with each other and with nearby crazes to produce the true crack. The crack itself runs primarily around but also through the dispersed phase. These features are consistent with the lower level of macroscopic dilation exhibited by these blends in comparison with their rubber-containing analogues.

5. Discussion

The foregoing results indicate that the deformation behaviour of toughened poly(phenylene oxide)–Nylon 6,6 blends is quite complex and exhibits several interesting features. Only elastic deformation is observed at low strains even when there is relatively poor interfacial adhesion. Above $\varepsilon_A = 1.5\%$ the deviatoric contribution to the overall strains begins to rise. Shear flow in the Nylon matrix is undoubtedly enhanced by the increased octahedral stress around the relatively soft poly(phenylene oxide)–rubber inclusions [1]. As

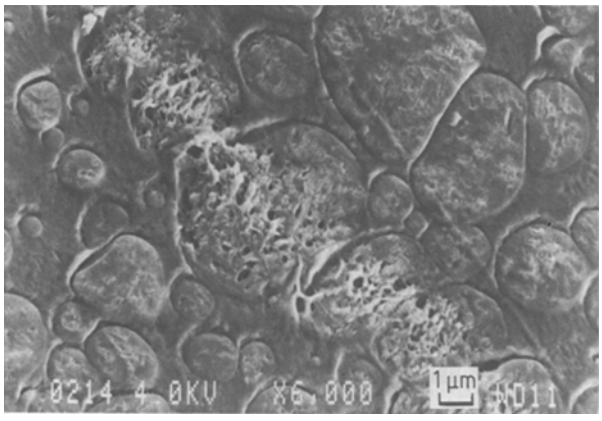

Figure 11 Scanning electron micrograph showing deformation band and internal cavitation in the dispersed poly(phenylene oxide) phase.

Figure 12 Higher magnification photograph of area shown in Fig. 10.

ε_A nears 2%, the initial signs of dilation occur. Although it was not possible to detect this dilation microscopically at such low strains, it seems clear from the photographs taken at higher strains that cavitation of the rubber or partial debonding of the poly(phenylene oxide) particles begins at this point. The process helps to relieve plane strain in the interior of the test specimens and further enhances shear flow in the Nylon matrix. Since cavitation remains contained within the dispersed phase, craze initiation in the Nylon is suppressed. This is a critical point in the deformation process because once sufficient plastic flow is established in the matrix resin, the material becomes extremely resistant to further craze development [7]. If no fracture occurs, mixed-mode deformation continues as the strain increases although ε_{DEV} rises at a faster rate than ε_{DIL}. Macroscopic shear banding was visible in some of the specimens tested to 14% strain. The presence of cavitated rubber in specimens broken at impact speeds implies that the

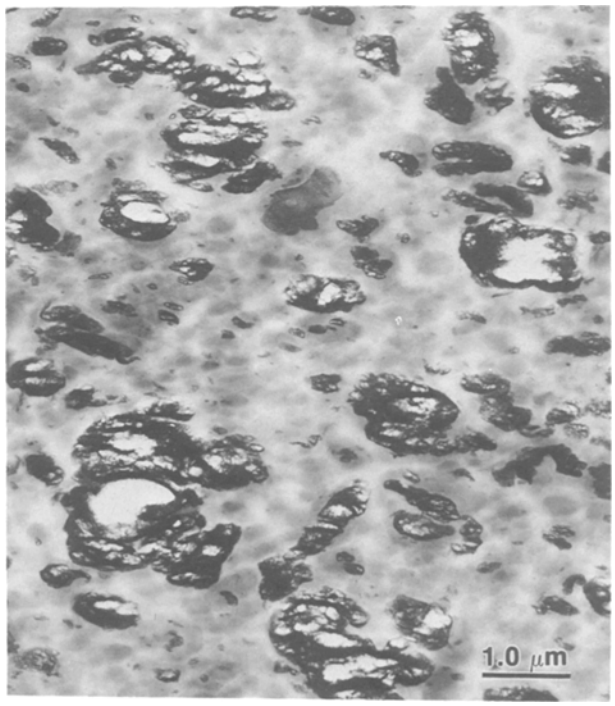

Figure 13 Transmission electron micrograph of subsurface deformation zone from an Izod fracture specimen. Note cavitation of the dispersed rubber.

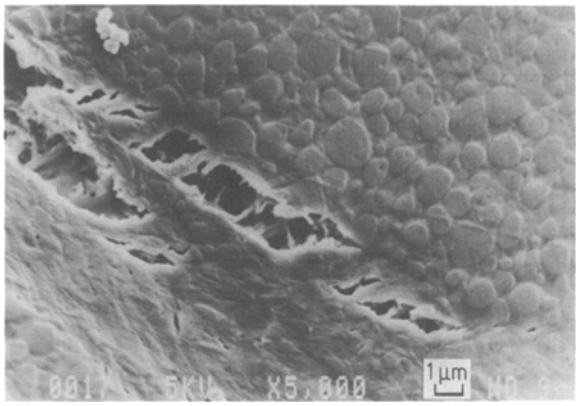

Figure 14 Scanning electron micrograph of crack tip poly(phenylene oxide)–Nylon 6,6 blend containing no rubber and showing an absence of cavitation in the dispersed phase.

deformation processes at low and high tests rates are similar. Substantial stress whitening is observed in both cases.

When rubber is absent from the system, the stress concentration around the dispersed particles drops and shear flow in the Nylon matrix occurs less readily. In addition, cavitation within the poly(phenylene oxide) phase becomes more difficult. These changes increase the probability of interfacial failure and the initiation of crazes at the particle equators. Craze breakdown occurs quite readily in Nylon 6,6 and the blends begin to exhibit brittle failure as the test speed is increased. This change is reflected in the volume strain and stress against strain curves for blends containing no rubber. The level of dilation and the elongation to break are substantially lower than in the toughened blends and show a more precipitous drop with increasing strain rate. In addition, stress whitening is absent.

Reductions in the copolymer concentration produce a somewhat different effect. Even at strain rates as low as 10^{-3}sec^{-1} brittle failure is observed at strains between 2 and 3%. There is no indication of enhanced dilation immediately before failure. Likewise very little stress whitening is visible on the fracture surfaces. These observations imply that the failure process is a very localized event with one craze in an immature craze field suddenly breaking down and giving way to rapid crack propagation. Since decreases in copolymer concentration result in substantial increases in particle size and a corresponding decrease in interfacial adhesion, it is difficult to assess which factor exerts the largest effect. Clearly, debonding from a large inclusion will produce a more serious defect than from a smaller one but it is not clear from these studies whether the poly(phenylene oxide) inclusions approach the critical flaw size for this system. It is worth noting that in the pigmented systems dilation occurs simultaneously with the onset of plastic flow while it is delayed in the unpigmented blends. This behaviour suggests that while the pigment may debond more readily than the poly(phenylene oxide), failures do not readily initiate from these voids. Some improvement in toughness with decreasing dispersed phase size is thus indicated. Other studies not reported in the current paper support this position.

The variation in the yield stress with log ($\dot{\varepsilon}$) is approximately linear for the blends examined in this study (see Fig. 10) and thus fits the criterion for a stress-activated viscous flow process. In the simplest case such behaviour can be described by the relationship

$$\sigma_y = E_A/V_A + (RT/V_A) \ln (\dot{\varepsilon}) \quad (4)$$

where E_A is an activation energy and V_A is an activation volume related to the number of polymer segments involved in the deformation process. For comparison purposes, the data for Nylon 6,6 homopolymer replotted from a recent paper by Hartman and Cole are included in Fig. 10 [8].

The complicated deformation behaviour of the blends precludes a rigorous interpretation of the difference between them and the Nylon homopolymer. Significantly, however, both the yield stress of poly(phenylene oxide) and its variation with strain rate are substantially higher than that of Nylon 6,6 [9]. This factor could be sufficient to produce the observed increase in the slope of the σ_{Ey} against $\dot{\varepsilon}$ curve for blends of the two resins. The increase may be further accentuated by a reduction in the molecular mobility of the Nylon segments which are chemically bound to the poly(phenylene oxide).

6. Conclusions

(1) In uniaxial tensile tests, ductile deformation is observed for all rubber-toughened poly(phenylene oxide)–Nylon 6,6 blends having more than 18% copolymer. Some breaks occur at the highest testing rates for blends having 10% copolymer. All blends having lower copolymer concentrations fail in a brittle manner at strains less than 3%.

(2) The measured volume strains for the ductile, rubber-toughened blends are significantly higher than for Nylon 6,6 homopolymer reaching a maximum value of approximately 3% at 10% strain. The cavitational component increases slowly with strain rate but never exceeds 20 to 25% of the total strain. Cavitation is confined primarily within the dispersed poly(phenylene oxide) particles. Photomicrographs of samples fractured at impact speeds demonstrate that the cavitation may be further confined to the rubber impact modifier in the dispersed phase.

(3) In the samples with less than 7% copolymer which fail at low strains, fracture is sudden and catastrophic with no measurable increase in dilation prior to the break. At the point of fracture, ε_{EL} comprises more than 90% of the total strain. The increased size and decreased adhesion of the dispersed phase facilitate the initiation and breakdown of matrix crazes.

(4) Blends with more than 15% copolymer containing no impact modifier show a marked drop in ductility as the testing rate is increased. The level of dilation also decreases significantly compared with blends containing rubber. Losses in toughness are attributed to reductions in the stress concentration around the poly(phenylene oxide) particles and the absence of a mechanism for controlled cavitation within the dispersed phase.

(5) The development of toughness in blends of poly(phenylene oxide)–Nylon depends strongly on the

interplay between several events. Shear flow in the Nylon matrix must be enhanced by softening the dispersed phase sufficiently to magnify the local stress field around the particles. Bonding between the two phases must be good enough that catastrophic craze breakdown does not short-circuit the plastic deformation process. Finally, cavitation must be allowed to develop but remain contained within the dispersed phase to reduce plane strain and allow time for shear flow of the matrix to become well established.

Acknowledgements

The authors are indebted to Dr J. C. Golba and his staff for providing the injection molded test specimens and to J. L. Methe for carrying out many of the volume strain measurements. The assistance of D. S. Matsumoto in modifying the graphical plotting routines used for displaying the data is greatly appreciated.

References

1. S. Y. HOBBS, M. E. J. DEKKERS and V. H. WATKINS, *J. Mater. Sci.*, submitted.
2. C. B. BUCKNALL and D. CLAYTON, *ibid.* **7** (1972) 202.
3. M. A. MAXWELL and A. F. YEE, *Pol. Eng. Sci.* 21 (1981) 205.
4. W. J. COUMANS, D. HEIKENS and S. D. SJOERDSMA, *Polymer* **21** (1981) 103.
5. D. HEIKENS, S. D. SJOERDSMA and W. J. COUMANS, *J. Mater. Sci.* **16** (1981) 429.
6. M. E. J. DEKKERS and D. HEIKENS, *J. Appl. Pol. Sci.* **30** (1985) 2389.
7. S. Y. HOBBS, R. C. BOPP and V. H. WATKINS, *Pol. Eng. Sci.* **23** (1983) 380.
8. B. HARTMAN and R. COLE Jr., *ibid.* **25** (1985) 65.
9. A. F. YEE, *ibid.* **17** (1977) 213.

Received 24 February
and accepted 18 July 1988